

## Fabrication of high-Q polydimethylsiloxane optical microspheres for thermal sensing

C.-H. Dong, L. He, Y.-F. Xiao, V. R. Gaddam, S. K. Ozdemir et al.

Citation: *Appl. Phys. Lett.* **94**, 231119 (2009); doi: 10.1063/1.3152791

View online: <http://dx.doi.org/10.1063/1.3152791>

View Table of Contents: <http://apl.aip.org/resource/1/APPLAB/v94/i23>

Published by the [American Institute of Physics](http://www.aip.org).

---

### Related Articles

Enhancing performance of polymer-based microlasers by a pedestal geometry  
*J. Appl. Phys.* **111**, 103116 (2012)

Strong coupling in monolithic microcavities with ZnSe quantum wells  
*Appl. Phys. Lett.* **100**, 161104 (2012)

Lens-less edge-pumped high power microchip laser  
*Appl. Phys. Lett.* **100**, 141105 (2012)

Directional waveguide coupling from a wavelength-scale deformed microdisk laser  
*Appl. Phys. Lett.* **100**, 061125 (2012)

Investigation of possible microcavity effect on lasing threshold of nonradiative-scattering-dominated semiconductor lasers  
*Appl. Phys. Lett.* **100**, 041105 (2012)

---

### Additional information on *Appl. Phys. Lett.*

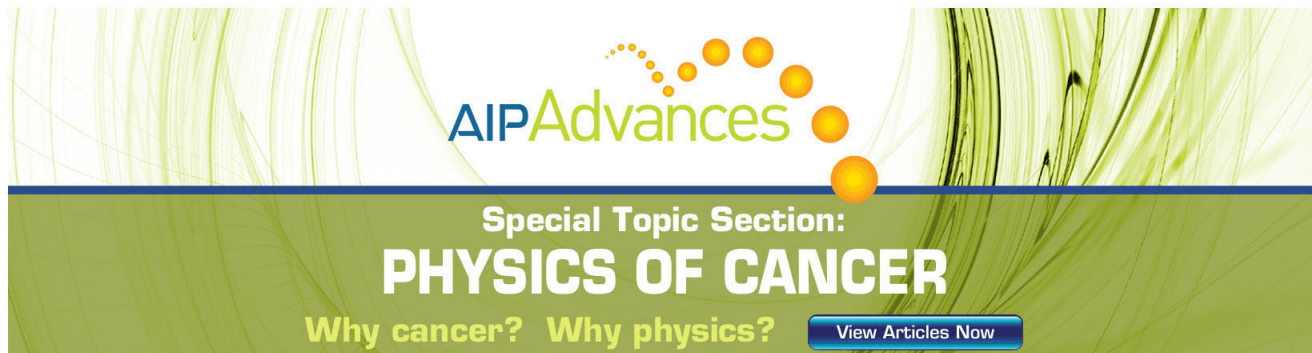
Journal Homepage: <http://apl.aip.org/>

Journal Information: [http://apl.aip.org/about/about\\_the\\_journal](http://apl.aip.org/about/about_the_journal)

Top downloads: [http://apl.aip.org/features/most\\_downloaded](http://apl.aip.org/features/most_downloaded)

Information for Authors: <http://apl.aip.org/authors>

## ADVERTISEMENT



**AIP Advances**

Special Topic Section:  
**PHYSICS OF CANCER**

Why cancer? Why physics? [View Articles Now](#)

## Fabrication of high- $Q$ polydimethylsiloxane optical microspheres for thermal sensing

C.-H. Dong,<sup>1,2</sup> L. He,<sup>1</sup> Y.-F. Xiao,<sup>1,3,a)</sup> V. R. Gaddam,<sup>1</sup> S. K. Ozdemir,<sup>1</sup> Z.-F. Han,<sup>2</sup> G.-C. Guo,<sup>2</sup> and L. Yang<sup>1,b)</sup>

<sup>1</sup>Department of Electrical and Systems Engineering, Micro/Nano Photonics and Photonic Materials Laboratory, Washington University in St. Louis, St. Louis, Missouri 63130, USA

<sup>2</sup>Key Laboratory of Quantum Information, University of Science and Technology of China, Hefei 230026, People's Republic of China

<sup>3</sup>State Key Laboratory for Artificial Microstructure and Mesoscopic Physics, School of Physics, Peking University, Beijing 100871, People's Republic of China

(Received 6 February 2009; accepted 20 May 2009; published online 10 June 2009)

Polydimethylsiloxane (PDMS) optical microspheres are fabricated and whispering gallery modes with quality factors of  $10^6$  in the 1480 nm band are demonstrated. The dependence of the resonance shifts on the input power is investigated in both the transient (blueshift) and the steady-state (redshift) regimes. Moreover, we demonstrate that such high- $Q$  PDMS optical resonators can be used as highly sensitive thermal sensors with temperature sensitivity of  $0.245 \text{ nm}/^\circ\text{C}$ , which is one order of magnitude higher than conventional silica microsphere resonators. The estimated thermal resolution of the sensor is  $2 \times 10^{-4} \text{ }^\circ\text{C}$ . © 2009 American Institute of Physics.

[DOI: 10.1063/1.3152791]

Whispering-gallery-mode (WGM) optical resonators with their high quality factors and small mode volumes have received considerable attention over the last decade, and they have become ideal platforms to study nonlinear phenomena and cavity quantum electrodynamics as well as highly sensitive optical detection and low-threshold lasing.<sup>1-7</sup> WGM microcavities made of inorganic materials, such as silica and silicon, have been intensively investigated in various geometries including spheres, disks and toroids. Many applications for these microcavities require further functionalization, flexibility, and larger nonlinearities that are difficult to achieve by traditional inorganic materials and processing techniques. The attributes of diversity, flexibility for processing and low cost make organic materials attractive and appropriate as alternative materials for high- $Q$  WGM resonators. Moreover, polymers have the potential for devices with advanced functionalities not attainable with inorganic materials. For example, in order to achieve thermal stability during continuous operation of silica microresonators, polymer coatings with negative thermo-optic coefficients have been proposed as a remedy to compensate the thermal induced redshift of the resonant wavelength.<sup>8,9</sup> Silica microspheres coated with a thin layer of polymer have found applications for optical switching and sensing.<sup>10,11</sup> A more interesting approach, on the other hand, would be to fabricate high- $Q$  microcavities using polymers only, without silicon/silica master.<sup>12</sup> Microspheres made of polymethyl methacrylate and polydimethylsiloxane (PDMS) have been fabricated and used for force and wall-shear stress measurements.<sup>13,14</sup>

In this paper, we investigate thermal effects in PDMS microspheres, and demonstrate their potential for highly sensitive thermal sensing. PDMS microspheres are fabricated without using a silica master structure or other soft lithographic molding techniques. PDMS is the material of choice,

owing to its low attenuation loss, good chemical stability, and large thermal nonlinearity. The PDMS microspheres were fabricated as explained in Ref. 13 with a slight modification. Instead of using a normal fiber, we used the tip of a tapered fiber which allowed us to prepare microspheres of smaller diameter. Specifically, the tip of a tapered fiber with diameter in the range of  $2\text{--}10 \mu\text{m}$  is inserted into and quickly withdrawn from a prepared PDMS liquid (RTV 184, Dow Corning 5:1). Due to surface tension, a spherical shaped PDMS cavity supported by the tapered fiber stem is formed with extremely smooth surface. By utilizing fiber tapers with different diameters and adjusting viscosity of the precured PDMS, microspheres with diameters ranging from  $100 \mu\text{m}$  to  $1 \text{ mm}$  can be prepared. The inset of Fig. 1(a) shows a typical microsphere with diameter ( $D$ ) of  $480 \mu\text{m}$ .

A tunable, single frequency, narrow linewidth ( $<300 \text{ kHz}$ ) external-cavity laser in the  $1460 \text{ nm}$  band is used to analyze the PDMS microsphere. The laser light is coupled into the microsphere through a fiber taper which also helps couple light out of the microsphere. The tapered section of the optical fiber is used to evanescently excite the WGMs in the PDMS microsphere. The coupling strength

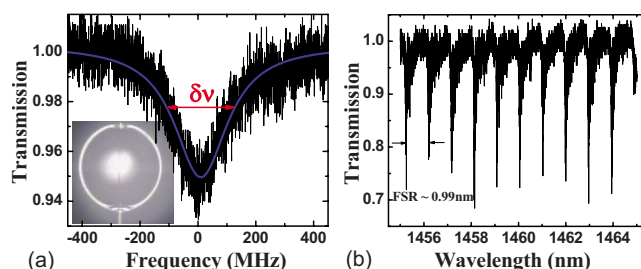


FIG. 1. (Color online) (a) Fine transmission spectrum of a WGM at  $1446.7 \text{ nm}$  which matches well with Lorentzian-shaped fitting line. The linewidth  $\delta\nu$  is about  $220 \text{ MHz}$ , corresponding to a loaded  $Q$  factor of  $9.1 \times 10^5$ . Inset: optical micrographs of PDMS microspheres with diameter  $D \sim 480 \mu\text{m}$ . (b) Transmission spectrum in  $1460 \text{ nm}$  band of the PDMS microsphere. The transmission dips correspond to the WGM resonances.

<sup>a)</sup>Electronic mail: yfxiao@pku.edu.cn.

<sup>b)</sup>Electronic mail: yang@ese.wustl.edu. URL: <http://ese.wustl.edu/~yang/>.

between the tapered fiber and the microsphere can be adjusted by changing the air gap between them. The output light is detected by a 125 MHz low-noise photo detector, which is connected to a digital oscilloscope to measure the transmission spectra.

Figure 1(a) depicts a single WGM at 1446.7 nm with a loaded  $Q$  factor up to  $10^6$ . Figure 1(b) shows a typical transmission spectrum where the dips correspond to the WGM resonances in the PDMS microsphere. The measured free spectrum range (FSR) describing the distance between two adjacent angular modes is about 0.99 nm, which is in good agreement with the theoretically calculated FSR  $\sim \lambda^2/(n\pi D)$ , where  $n=1.41$  is the refractive index of the PDMS.<sup>15</sup> Due to the small eccentricity ( $\sim 2.1\%$ ) of the microsphere, the degeneracy of the WGMs with the same angular but different azimuthal mode numbers are lifted, resulting in a fine feature around each dip, as shown in Fig. 1(b).

The thermal effect of the WGMs in the microsphere results from temperature-induced changes both in the refractive index of the PDMS and in the diameter of the microcavity. Resonant wavelength shift  $\Delta\lambda$  can be expressed as

$$\Delta\lambda = \lambda_0 \left( \frac{1}{n} \frac{dn}{dT} \Delta T + \frac{1}{D} \frac{dD}{dT} \Delta T \right), \quad (1)$$

where  $dn/dT = -10^{-4} \text{ K}^{-1}$  is the coefficient of thermal refraction of PDMS and  $(1/D)(dD/dT) = 2.7 \times 10^{-4} \text{ K}^{-1}$  is the coefficient of thermal expansion.  $\lambda_0$  designates the cold cavity resonant wavelength and  $\Delta T$  denotes the temperature change of the PDMS microcavity. According to Eq. (1), the thermal refraction of PDMS causes blueshift of the WGMs, while the thermal expansion compels a redshift when  $\Delta T > 0$ . Response time of thermal refraction is typically tens of microsecond, while the response time of thermal expansion is much longer (more than tens of milliseconds).<sup>16,17</sup> To clarify the effect of these different response times on thermodynamics of the WGM, we performed two experiments in both transient and steady-state regimes.

In the first experiment, we scanned the WGM to study the thermal effect in the transient regime. Figure 2(a) shows the measured resonant wavelength shift as a function of the pump power when the WGM is scanned at a frequency of 10 Hz (scanning rate: 4 nm/s). Unlike in the pure silica microcavity,<sup>18</sup> the wavelength shift here exhibits a blueshift with increasing excitation (pump) power. This can be explained by the negative coefficient of thermal refraction of PDMS. When the excitation laser is launched into the microcavity, it heats the microcavity ( $\Delta T > 0$ ). Due to the very short transit time ( $< 10$  ms) when the scanning wavelength passes through the cavity mode, the thermal refraction effect is dominant in the scanning because it responds much faster (tens of microseconds) than the thermal expansion effect (of the order of seconds). It has no enough time to respond and manifest itself in the WGM for the thermal expansion effect.<sup>15-17,19</sup> Therefore, the system cannot reach thermal equilibration. As a result, the measured resonant wavelength of the WGM experiences a blueshift while in silica microresonator it is a redshift. This blueshift explains the reason for the broadening (compression) of transmission dip during down (up)-scan of the wavelength, shown in the inset of Fig. 2(a). It is worth noting that the points plotted in Fig. 2(a) correspond to the shift of the resonance dip in the wavelength downscan.

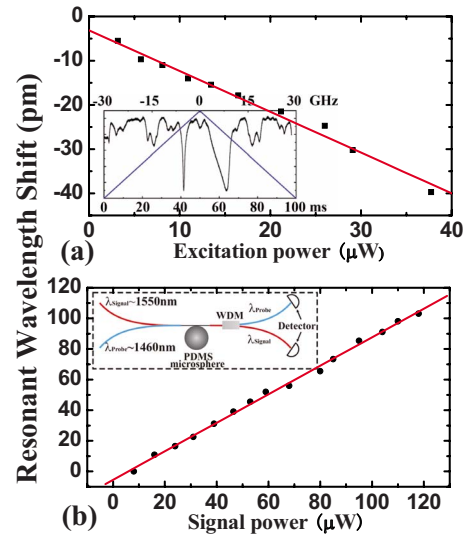


FIG. 2. (Color online) (a) Resonant wavelength shift vs excitation power. Inset shows two transmission dips corresponding to the same resonant mode, but with up- and down-wavelength scanings (blue line), respectively. The scanning frequency is 10 Hz. Here, the upper and bottom axis denote frequency and time, respectively. (b) Resonant wavelength shift of the probe WGM ( $\lambda_0=1446.7$  nm) vs the signal power. Inset shows the schematic of the experimental setup. WDM: wavelength-division multiplexing. The red lines are linear fittings of the experimental data.

In the second experiment we introduced two lasers in the measurements. One is a very weak probe wave exciting a high- $Q$  WGM at 1446.7 nm ( $\sim 5 \mu\text{W}$ , small enough to minimize its self-thermal effect) with a fine scanning frequency of 100 Hz (40 nm/s). The pump (signal) wave in 1550.0 nm band is tuned (no wavelength scanning) to continually excite a low- $Q$  ( $\sim 10^3$ ) WGM due to the fact that the linewidth of the laser is much narrower than the low- $Q$  mode's, as shown in the inset of Fig. 2(b). With this configuration, we can quantitatively study how the resonant wavelength of the probe shifts with the varying input power of the pump by recording the resonant wavelength of the probe WGM. Figure 2(b) depicts the wavelength shift of the probe WGM as a function of the absorbed signal power. Unlike Fig. 2(a), it exhibits an obvious redshift with increased signal power, which results from both the thermal refraction and the thermal expansion of PDMS. Since we do not scan the pump light, the PDMS microsphere can reach thermal equilibration after a sufficient duration of time. As a result, the thermal expansion becomes dominant due to the larger absolute value of thermal expansion coefficient (positive) than thermal refraction coefficient (negative).

The result in Fig. 2(b) demonstrates a potential application of the PDMS microsphere toward highly sensitive thermal sensing. The pump light actually plays the role of a heater. In other words, it simulates the temperature variation of the surrounding. In order to directly demonstrate the thermal response of the PDMS microsphere in an actual setting, we placed a heater and a thermometer in an enclosed space, and recorded the shifts in the resonance wavelength of the WGM as the power of the heater is slowly increased. Figure 3 shows the resonant wavelength shift of the probe WGM as a function of the surrounding temperature. When the temperature of the surrounding is slowly increased from room temperature to 32 °C, the resonant wavelength shows a redshift of  $\sim 2.4$  nm. The sensitivity curve exhibits an excellent

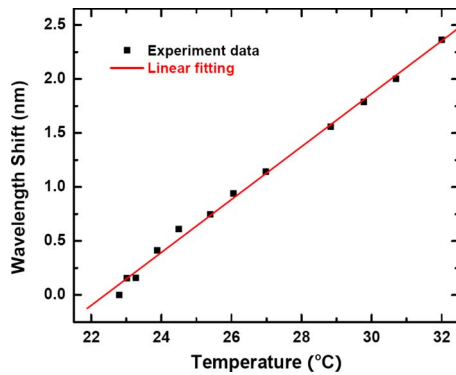


FIG. 3. (Color online) Resonant wavelength shift of the WGM as a function of surrounding temperature.

linearity in the range of temperature change, with a slope of  $0.245 \text{ nm}/^\circ\text{C}$  which agrees well with the predicted theoretical value of  $0.285 \text{ nm}/^\circ\text{C}$  using Eq. (1). Taking into account the spectral resolution<sup>7</sup> of our system, which is  $\sim 0.05 \text{ pm}$ , we estimate the resolution of the PDMS microsphere temperature sensor as  $2 \times 10^{-4} \text{ }^\circ\text{C}$ .

Large coefficients of thermal refraction and expansion of PDMS make these microspheres much more sensitive to temperature changes than their silica counterparts.<sup>20–22</sup> The reported sensitivity of a silicon microring resonator temperature sensor is  $0.11 \text{ nm}/^\circ\text{C}$ ,<sup>23</sup> which is less than half of the sensitivity of the PDMS microsphere. The fabricated PDMS microsphere has a better resolution than other reported resonance-based temperature sensors, such as surface plasmon resonance<sup>24,25</sup> and on-chip Fabry–Pérot resonator.<sup>26</sup> While some of the reported interferometric temperature sensors<sup>27–32</sup> have better sensitivities ( $0.99\text{--}3.195 \text{ nm}/^\circ\text{C}$ ) than the PDMS microsphere, their resolutions ( $3.4 \times 10^{-3}\text{--}0.4 \text{ }^\circ\text{C}$ ) are smaller than that of the PDMS microsphere. A drawback of PDMS microsphere as a temperature sensor is its limited operating range of  $-50\text{--}200 \text{ }^\circ\text{C}$  which is much lower than that of optical fiber interferometric temperature sensors with demonstrated operations at temperatures as high as  $1200 \text{ }^\circ\text{C}$ .<sup>30–32</sup>

In summary, we have fabricated high- $Q$  PDMS microspheres using a simple but highly efficient method, and investigated the thermal effect of WGMs in detail. A  $Q$ -factor of  $10^6$  corresponding to a linewidth of  $1.5 \text{ p.m.}$  is obtained regularly at  $1450 \text{ nm}$  band. Observed high thermal sensitivity ( $0.245 \text{ nm}/^\circ\text{C}$ ) and high temperature resolution ( $2 \times 10^{-4} \text{ }^\circ\text{C}$ ), ease of fabrication, and the compact structure make high- $Q$  PDMS microspheres a promising candidate for temperature sensing.

C.-H.D. and L.H. contributed to this work equally. The authors gratefully acknowledge I-CARES (International

Center for Advanced Renewable Energy and Sustainability) and CMI (Center for Materials Innovation) at Washington University for support of this work. Yun-Feng Xiao was also supported by the Research Fund for the Doctoral Program of Higher Education, the Scientific Research Foundation for the Returned Overseas Chinese Scholars, and the National Natural Science Foundation of China under Grant No. 10821062, and the National Basic Research Program of China under Grant Nos. 2006CB921601 and 2007CB307001.

<sup>1</sup>K. J. Vahala, *Nature (London)* **424**, 839 (2003).

<sup>2</sup>I. H. Agha, Y. Okawachi, M. A. Foster, J. E. Sharping, and A. L. Gaeta, *Phys. Rev. A* **76**, 043837 (2007).

<sup>3</sup>Y.-F. Xiao, Z.-F. Han, and G.-C. Guo, *Phys. Rev. A* **73**, 052324 (2006).

<sup>4</sup>L. Yang, D. K. Armani, and K. J. Vahala, *Appl. Phys. Lett.* **83**, 825 (2003).

<sup>5</sup>C.-H. Dong, Y.-F. Xiao, Z.-F. Han, G.-C. Guo, X.-S. Jiang, L.-M. Tong, C. Gu, and H. Ming, *IEEE Photon. Technol. Lett.* **20**, 342 (2008).

<sup>6</sup>F. Vollmer, D. Braun, A. Libchaber, M. Khoshshima, I. Teraoka, and S. Arnold, *Appl. Phys. Lett.* **80**, 4057 (2002).

<sup>7</sup>N. M. Hanumegowda, C. J. Stica, B. C. Patel, I. White, and X. Fan, *Appl. Phys. Lett.* **87**, 201107 (2005).

<sup>8</sup>M. Han and A. Wang, *Opt. Lett.* **32**, 1800 (2007).

<sup>9</sup>L. He, Y. Xiao, C. Dong, J. Zhu, V. Gaddam, and L. Yang, *Appl. Phys. Lett.* **93**, 201102 (2008).

<sup>10</sup>H. C. Tapalian, J.-P. Laine, and P. A. Lane, *IEEE Photon. Technol. Lett.* **14**, 1118 (2002).

<sup>11</sup>I. Teraoka and S. Arnold, *J. Opt. Soc. Am. B* **24**, 653 (2007).

<sup>12</sup>C.-Y. Chao and L. J. Guo, *Appl. Phys. Lett.* **83**, 1527 (2003).

<sup>13</sup>T. Ioppolo, U. K. Ayaz, M. V. Ötügen, and V. Sheverev, 46th AIAA Aerospace Sciences Meeting and Exhibit 2008-273 (2008).

<sup>14</sup>T. Ioppolo, T. M. Kozhevnikov, M. V. Ötügen, and V. Sheverev, 45th AIAA Aerospace Sciences Meeting and Exhibit 2007-1262 (2007).

<sup>15</sup>B. A. Grzybowski, S. T. Brittain, and G. M. Whitesides, *Rev. Sci. Instrum.* **70**, 2031 (1999).

<sup>16</sup>T. Gensch and C. Viappiani, *Photochem. Photobiol. Sci.* **2**, 699 (2003).

<sup>17</sup>A. Maznev, J. Hohlfield, and J. Güdde, *J. Appl. Phys.* **82**, 5082 (1997).

<sup>18</sup>T. Carmon, L. Yang, and K. J. Vahala, *Opt. Express* **12**, 4742 (2004).

<sup>19</sup>C. Schmidt, A. Chipouline, T. Pertsch, A. Tünnermann, O. Egorov, F. Lederer, and L. Deych, *Opt. Express* **16**, 6285 (2008).

<sup>20</sup>J. D. Suter, I. M. White, H. Zhu, and X. Fan, *Appl. Opt.* **46**, 389 (2007).

<sup>21</sup>T. Le, A. Savchenkov, N. Yu, L. Maleki, and W. H. Steier, *Appl. Opt.* **48**, 458 (2009).

<sup>22</sup>Q. Ma, T. Rossmann, and Z. Guo, *J. Phys. D* **41**, 245111 (2008).

<sup>23</sup>M. S. Nawrocka, T. Liu, X. Wang, and R. R. Panepucci, *Appl. Phys. Lett.* **89**, 071110 (2006).

<sup>24</sup>H. P. Chiang, C.-W. Chen, J. J. Wu, H. L. Li, T. Y. Lin, E. J. Sanchez, and P. T. Leung, *Thin Solid Films* **515**, 6953 (2007).

<sup>25</sup>S. K. Özdemir and G. Turhan-Sayan, *J. Lightwave Technol.* **21**, 805 (2003).

<sup>26</sup>G. Cocorullo, F. G. Della Corte, M. Iodice, I. Rendina, and P. M. Sarro, *IEEE Trans. Electron Devices* **44**, 766 (1997).

<sup>27</sup>A. N. Starodumov, L. A. Zenteno, D. Monzon, and E. De La Rosa, *Appl. Phys. Lett.* **70**, 19 (1997).

<sup>28</sup>E. Li and G.-D. Peng, *Opt. Commun.* **281**, 5768 (2008).

<sup>29</sup>S.-L. Tsao and P.-C. Peng, *Microwave Opt. Technol. Lett.* **30**, 321 (2001).

<sup>30</sup>H.-S. Choi, H. F. Taylor, and C. E. Lee, *Opt. Lett.* **22**, 1814 (1997).

<sup>31</sup>Y. Zhu and A. Wang, *Appl. Opt.* **45**, 6071 (2006).

<sup>32</sup>H. Y. Choi, K. S. Park, S. J. Park, U.-C. Paek, B. H. Lee, and E. S. Choi, *Opt. Lett.* **33**, 2455 (2008).